CRETE 2017:

Understanding jet launching through polarization observations.

RadioNet has received funding from the European Union’s Horizon 2020 research and innovation programme under grant agreement No 730562

CRETE 2017:

~~Understanding jet launching through polarization observations.~~

(1) Cores and opacity: effect on polarization

(2) Review some of what’s new in jet polarization

(3) New images and more on 3C 273

(4) Currents in jets

(1) CORES AND OPACITY

Shocking news! The EVPA does not flip by 90 degrees at tau = 1

(1) CORES AND OPACITY

Shocking news! The EVPA does not flip by 90 degrees at tau = 1

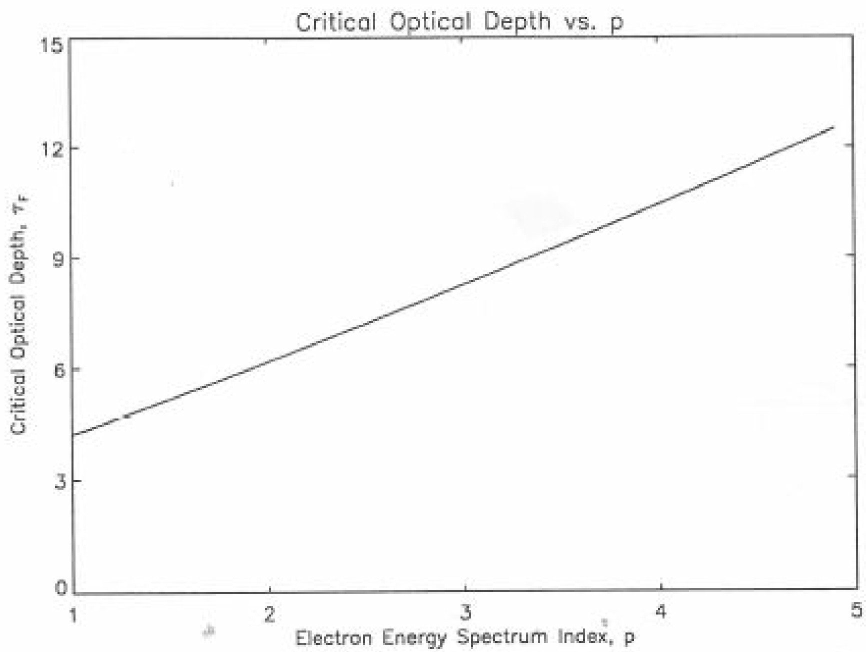

Figure 3.2: Critical optical depth at which the polarization 'flips' through 90° as a function of electron spectral index for Faraday thin slabs.

BURN 1966

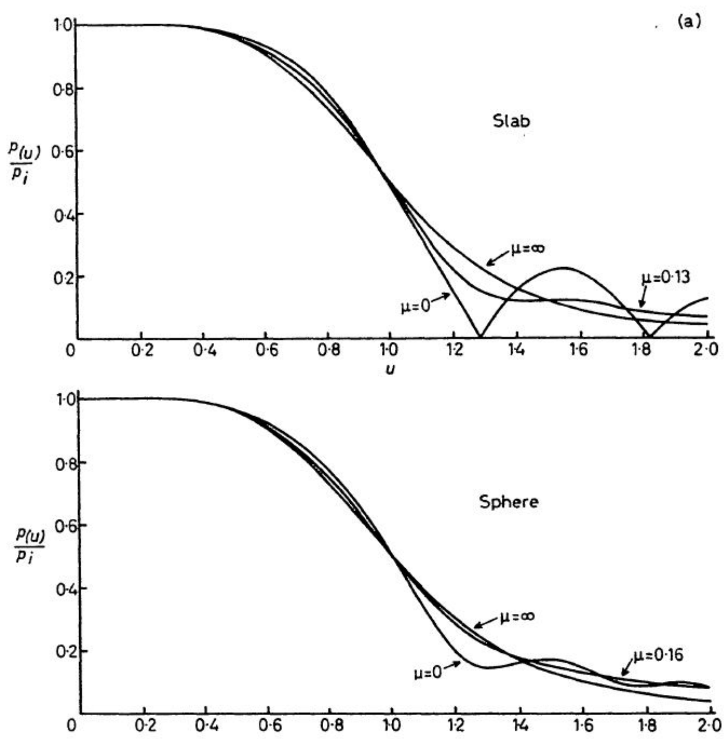

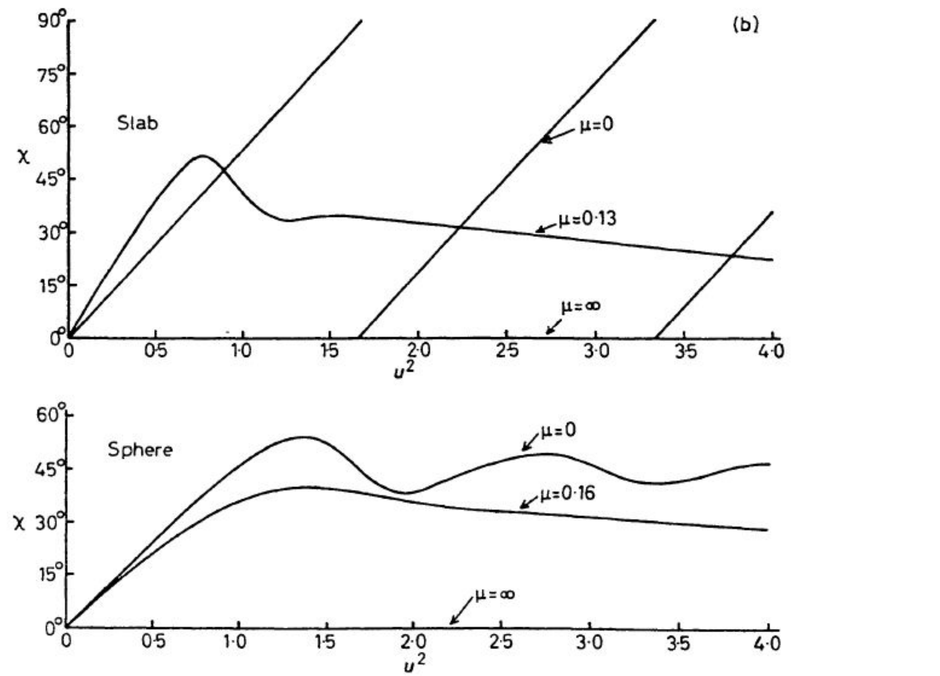

FIG. 2. *Polarization of models of internal Faraday dispersion.* (*a*) *Degree of polarization* (*b*) *angle of polarization.*

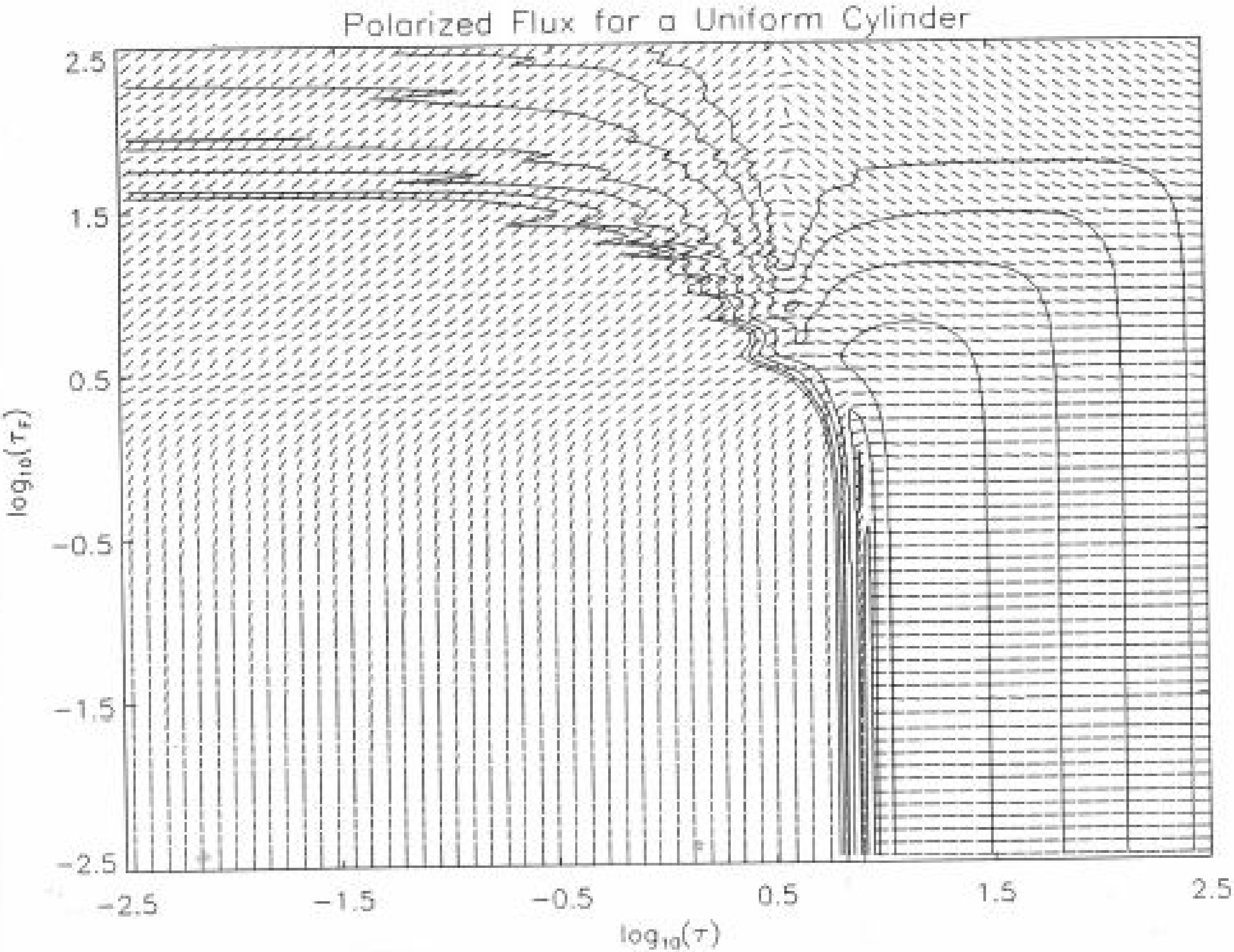

Polarized Flux for a Uniform Cylinder
2.5
1.5
0.5
−0.5
−1.5
−2.5
$\log_{10}(\tau_F)$
−2.5
−1.5
−0.5
0.5
1.5
2.5
$\log_{10}(\tau)$

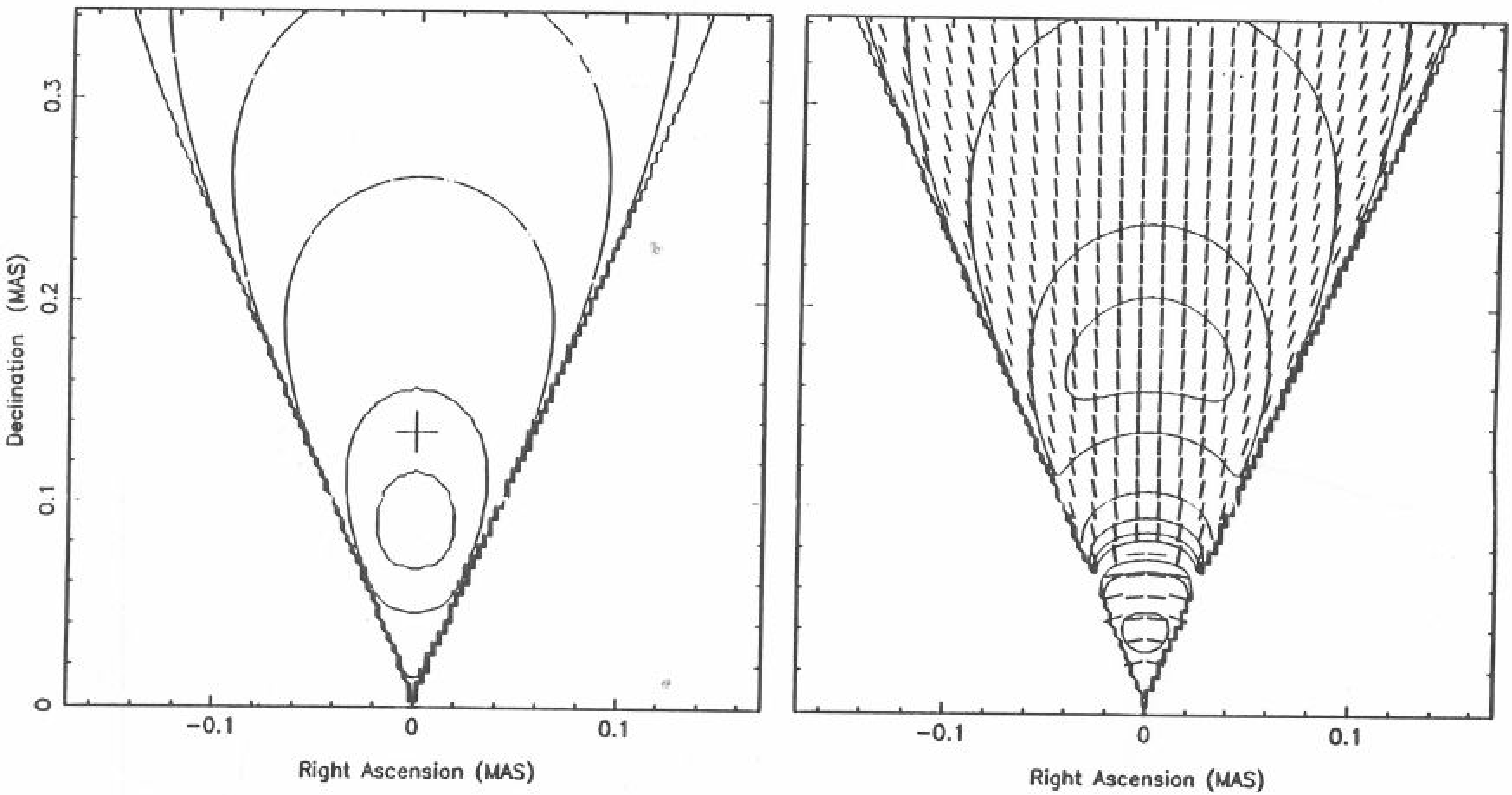

Figure 4.1: I and P maps corresponding to the jet Königl's 1981 paper. The cross on the I map marks the location of the position of the optical surface along the jet's axis.

MOTTER and GABUZDA 2017

“18-22 cm VLBA Faraday rotation studies of 6 AGN jets”

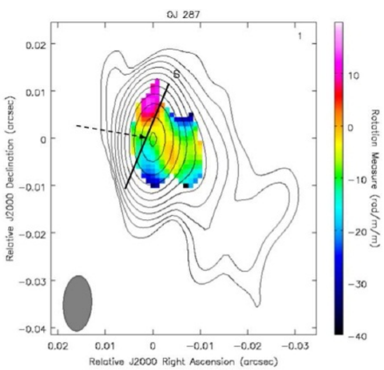

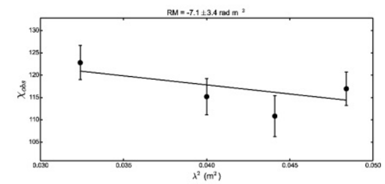

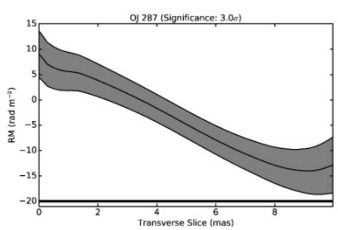

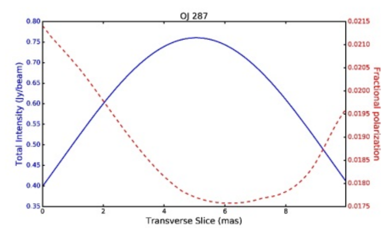

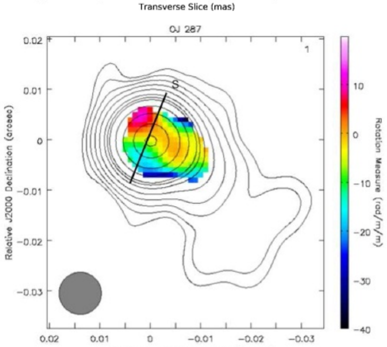

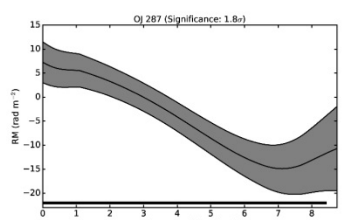

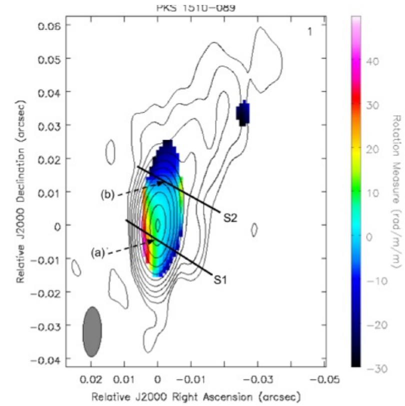

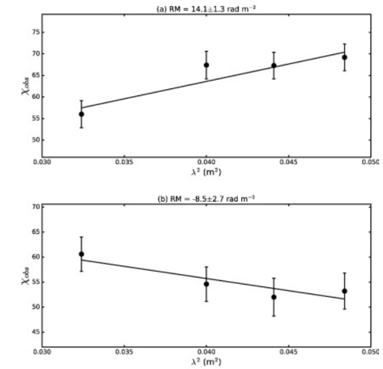

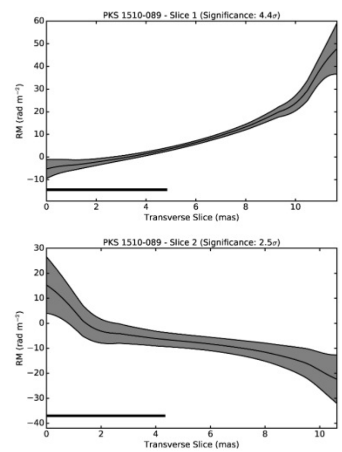

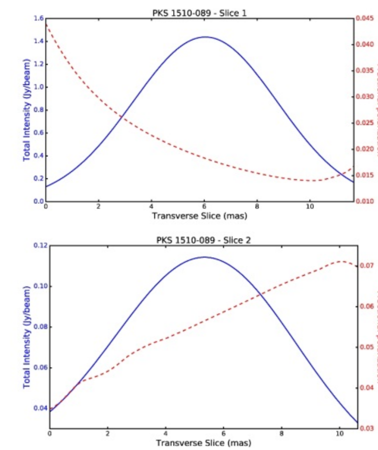

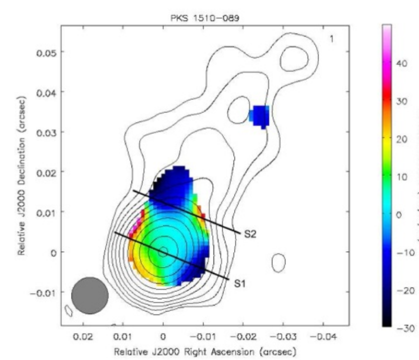

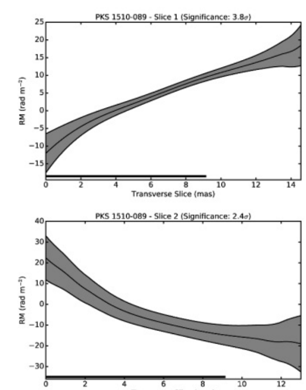

(2) OTHER NEW PAPERS ON JET POLARIZATION

Kravchenko, Kovalev and Sokolovsky 2017

“Parsec scale Faraday rotation and polarization of 20 active galactic nuclei jets”

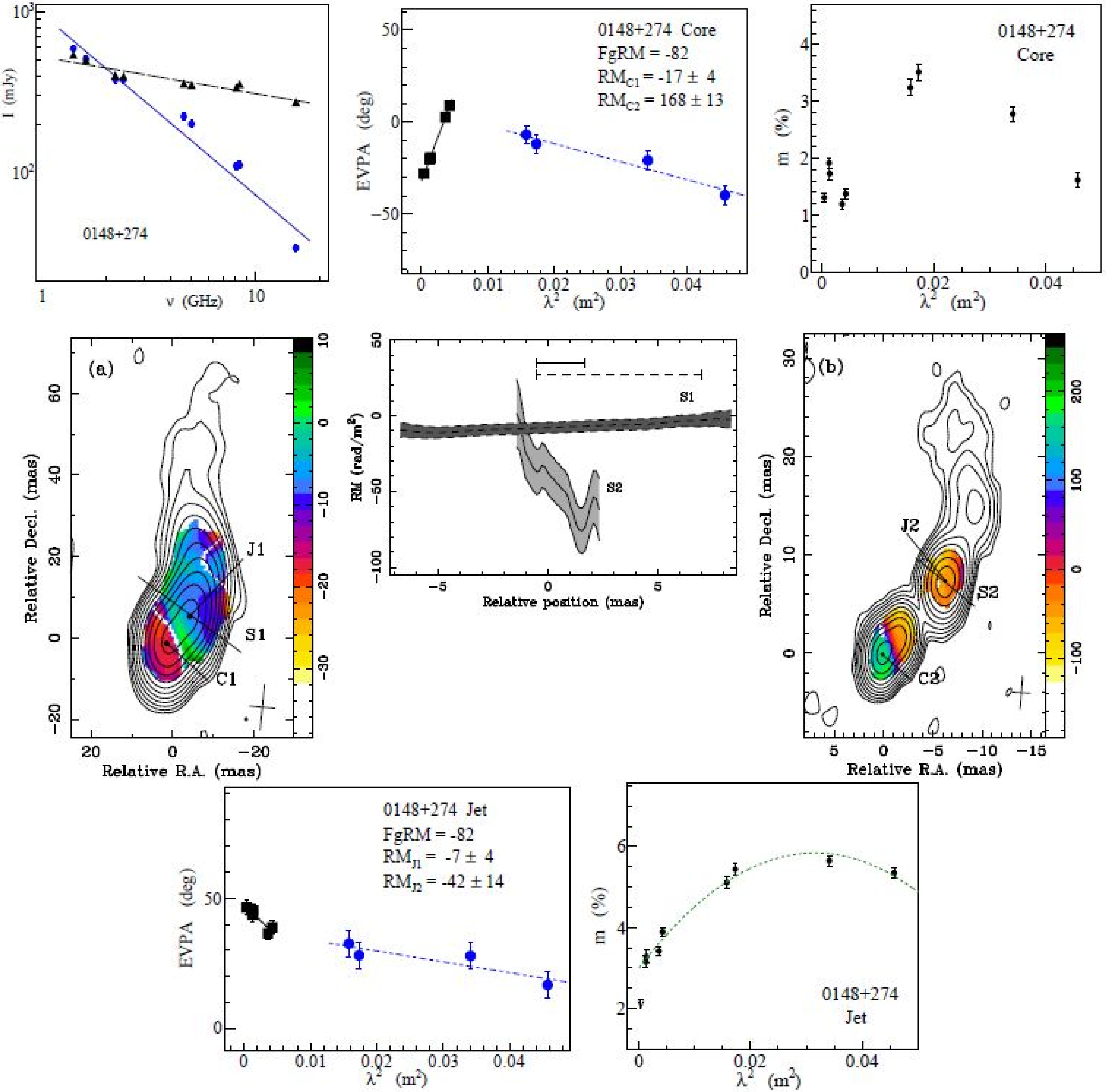

Figure 3.1. Source 0148+274. (a) 1.4 GHz to 2.4 GHz Faraday RM map in the observer's frame. (b) 4.6 GHz to 15.4 GHz RM map.

Kiehlmann +++ 2016

“Polarization angle swings in blazars: The case of 3C 279”

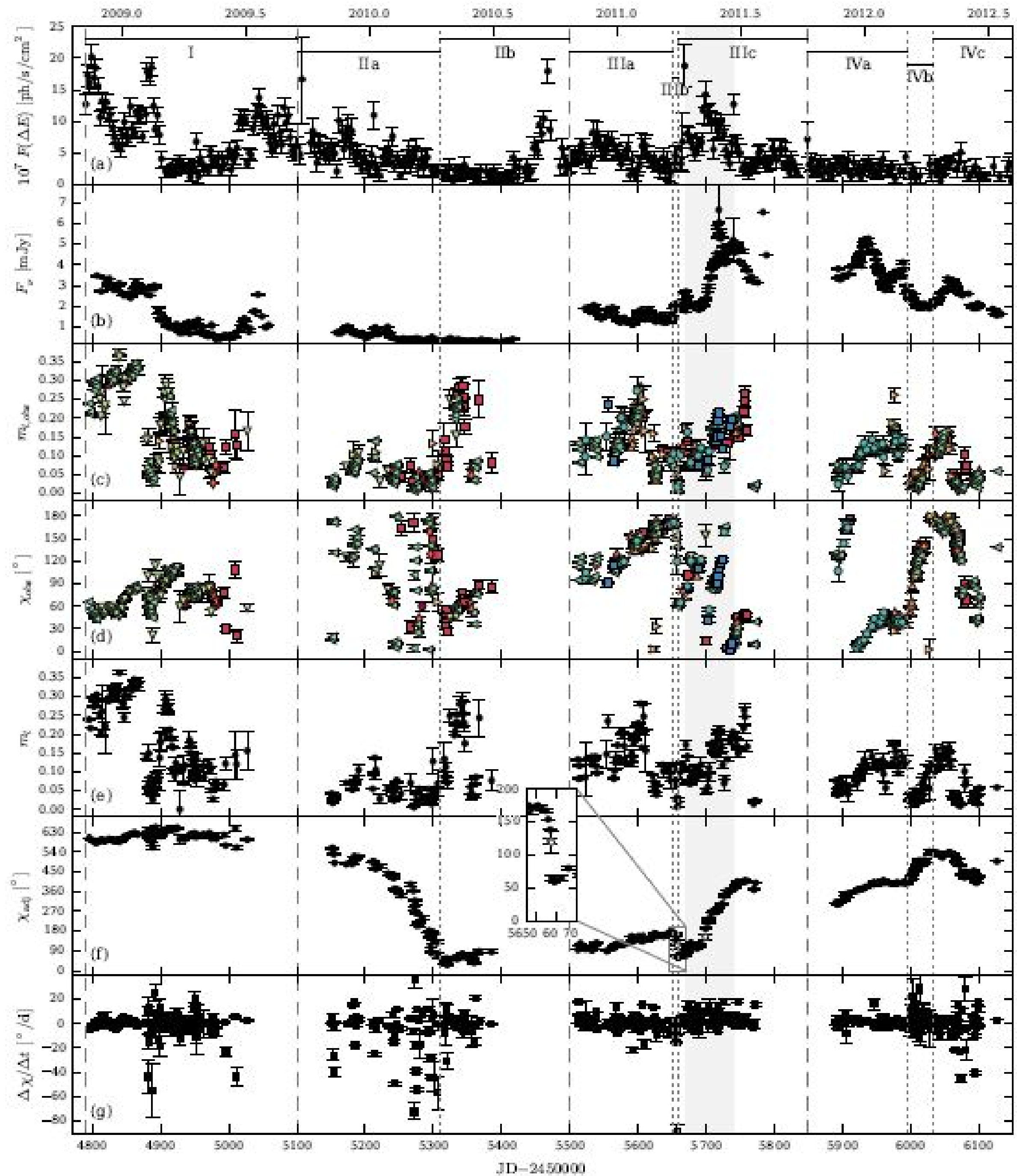

Fig. 1. Optical photometry and polarimetry and γ-ray light curve of 3C 279. *Fermi*-LAT γ-ray light curve at >100 MeV binned into 3 day intervals

Lyutikov and Kravchenko 2017

“Polarization swings in blazars”

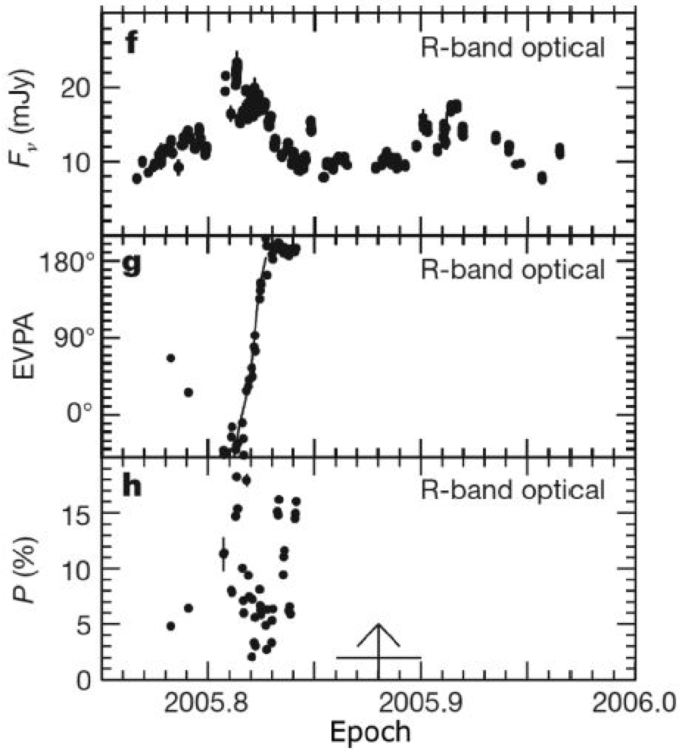

Figure 1 Optical *R*-band observations of BL Lac as functions of time, (*f*) flux density, (*g*) degree of polarization and (*h*) EVPA (see fig. 2 of Marscher et al. 2008).

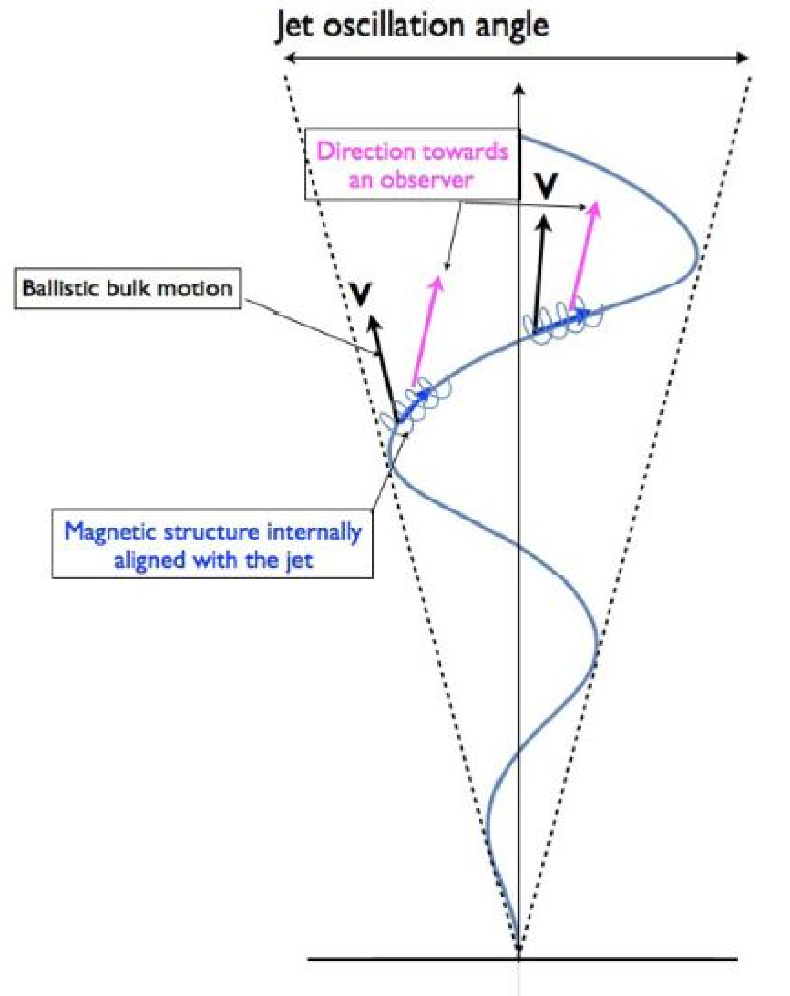

Figure 2. Schematic representation of the model. The jet is emitted along a variable direction (defined, e.g. by the opening angle of the planar motion, jets' oscillation angle). The internal helical structure of the magnetic field within the jet is aligned with the local jet direction and changes with time.

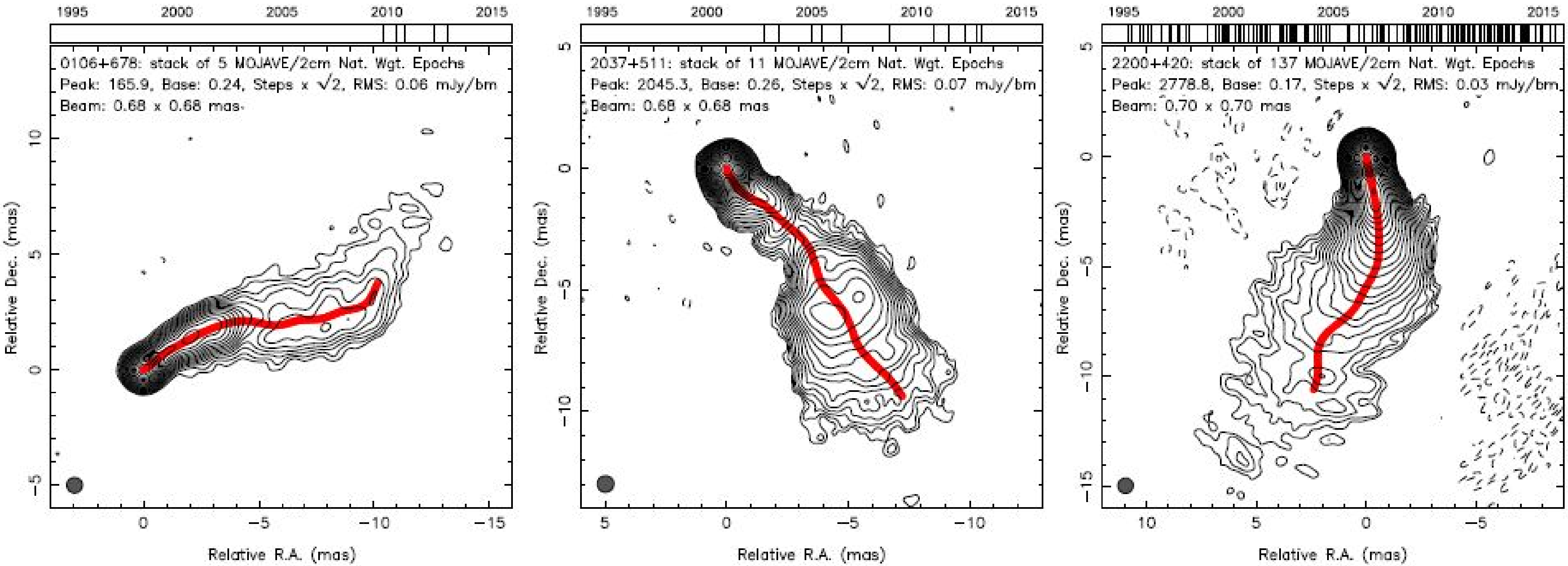

Pushkarev, Kovalev, Lister and Savolainen 2017 "MOJAVE – XIV. Shapes and opening angles of AGN jets"

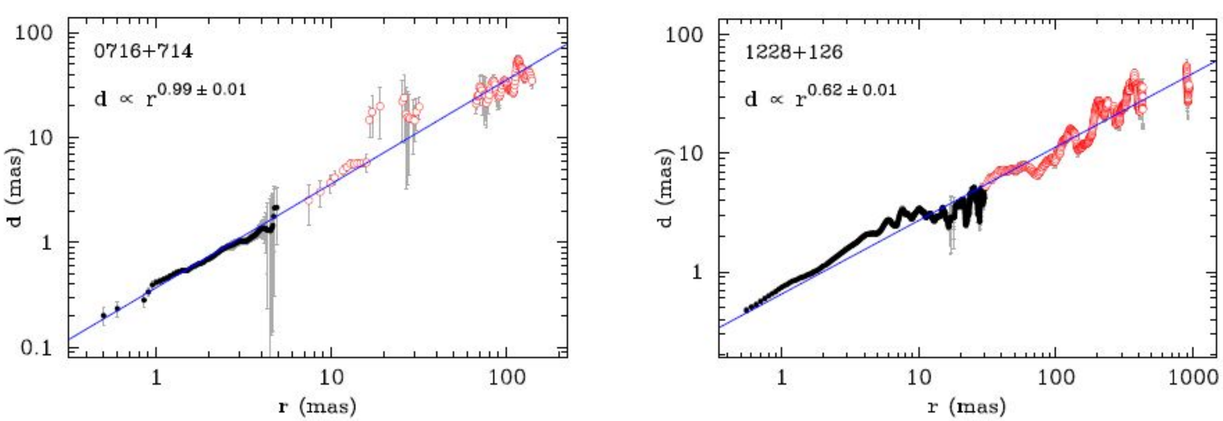

Figure 7. Transverse jet width versus a distance along ridge line for the BL Lac object 0716+714 (left-hand panel) and radio galaxy M87 (right-hand panel)

Mościbrodzka, Dexter, Davelaar and Falcke 2017 “Faraday rotation in GRMHD simulations of the jet Launching zone of M87”

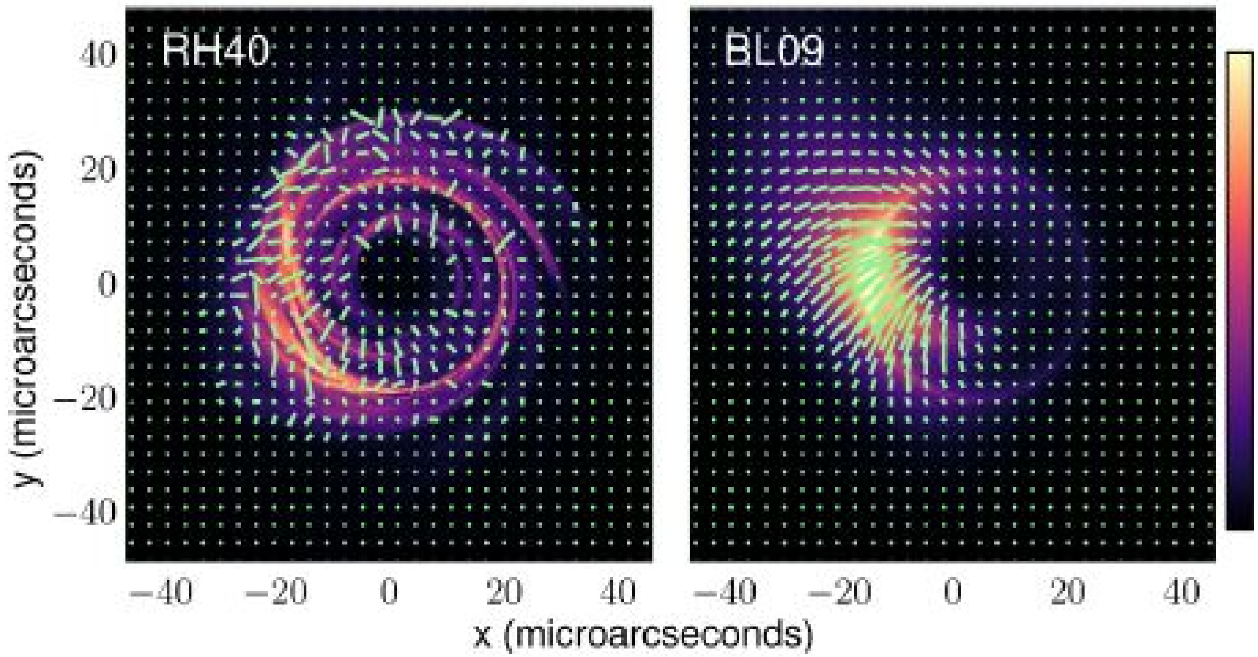

Figure 4. Intensity (colours) and polarization maps (ticks) for model RH40 (left) and a semi-analytic force-free jet model (right, Broderick & Loeb 2009; hereafter BL09). Each image is scaled linearly to its maximum intensity. The strong Faraday rotation through the accretion disc leads to a scrambled polarization pattern in the RH40 case, while the force-free jet shows coherent polarization that traces its helical magnetic field structure. The BL09 model has a much higher net polarization ($\simeq$15 per cent compared to $\simeq$1 per cent for RH40), which is not seen in SMA observations of M87* (Kuo et al. 2014).

Gold, McKinney, Johnson and Doeleman 2017

“Probing the Magnetic Field Structure in Sgr A* on Black Hole Horizon Scales with Polarized Radiative Transfer Simulations”

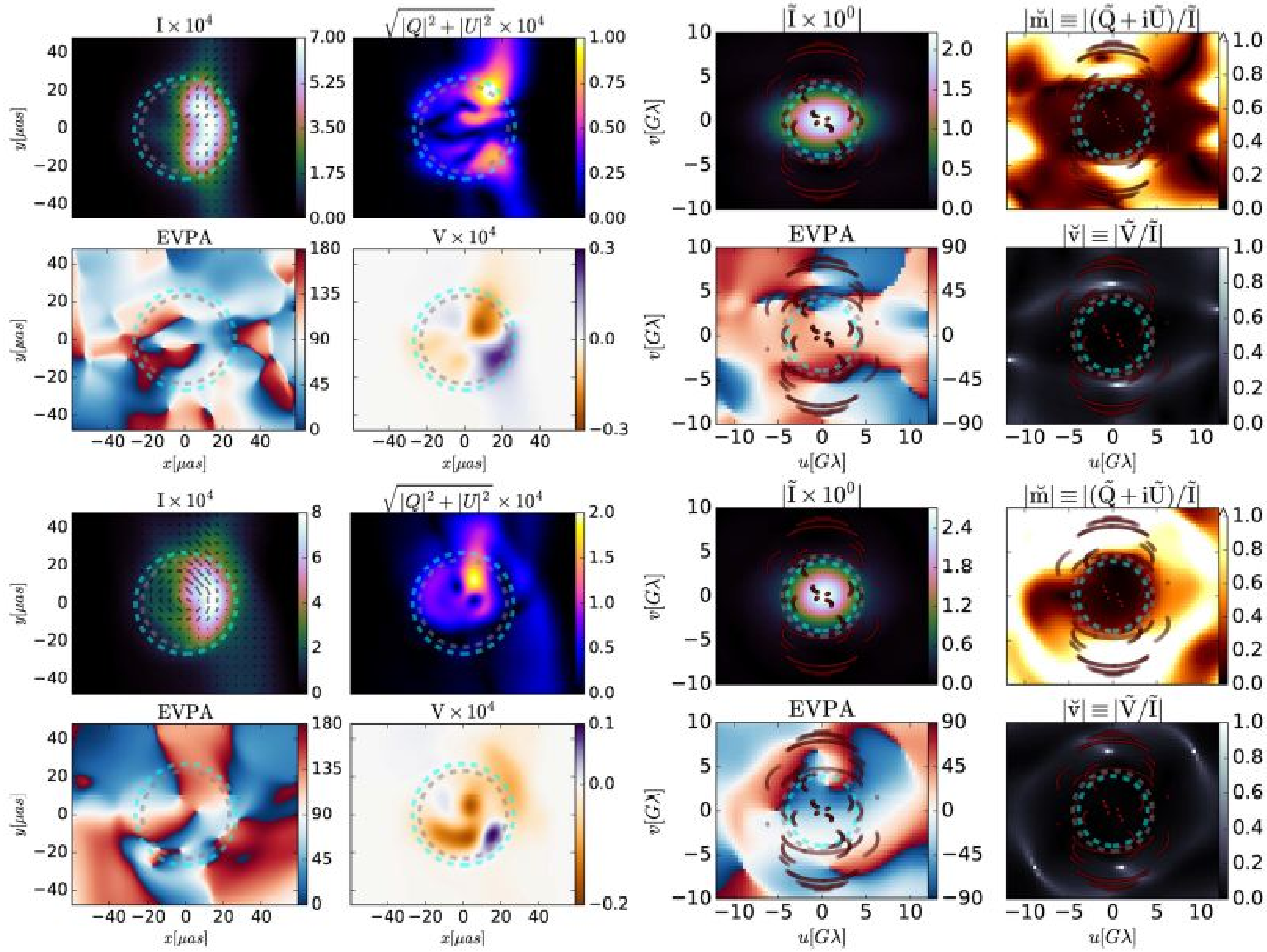

Zhang, Li, Guo and Taylor 2017

"Polarization Signatures of Kink Instabilities in the Blazar Emission Region from Relativistic Magnetohydrodynamic Simulations"

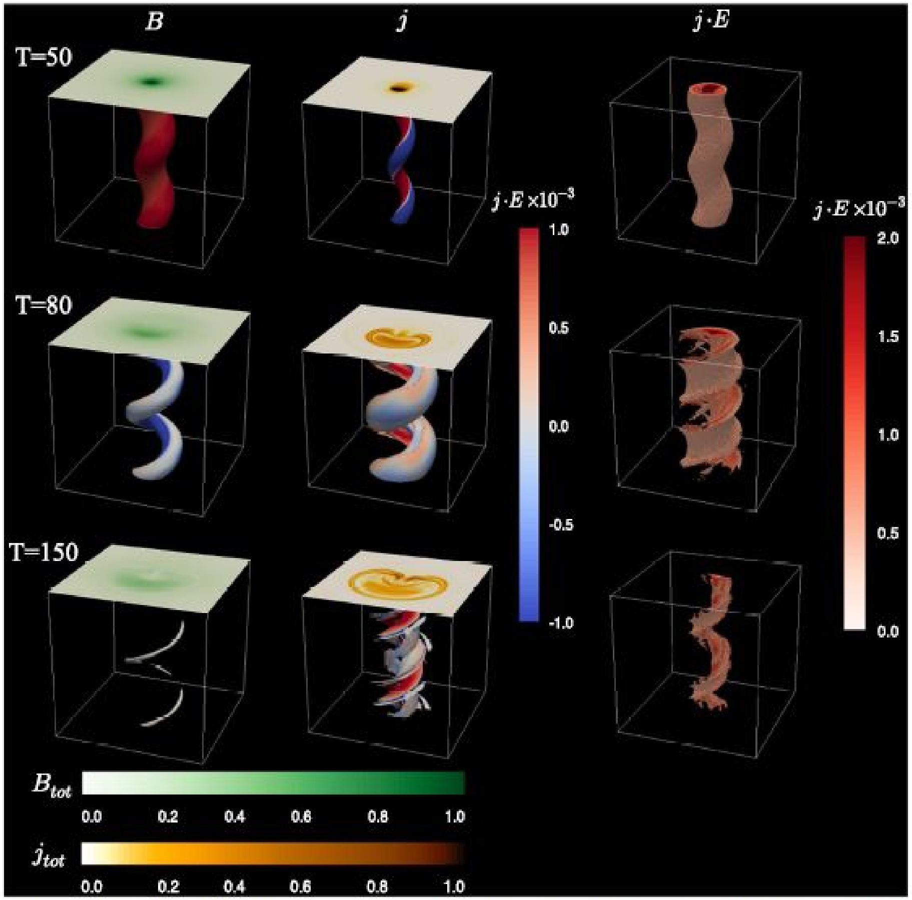

Figure 2. Kink evolution for Case 1. Left column is the 3D isosurface of the magnetic field strength at $B = 0.2$, with the transverse slice at the top of the simulation box. Middle column is those for the magnitude of the current density, with the isosurface chosen at $|j| = 0.2$. The color on both isosurfaces present the distribution of $\boldsymbol{j} \cdot \boldsymbol{E}$. Right column plots all zones with a positive $\boldsymbol{j} \cdot \boldsymbol{E}$, and the color indicates the strength of $\boldsymbol{j} \cdot \boldsymbol{E}$. Panels are selected at code units $T = 50$ (upper row), $T = 80$ (middle row), and $T = 150$ (lower row).

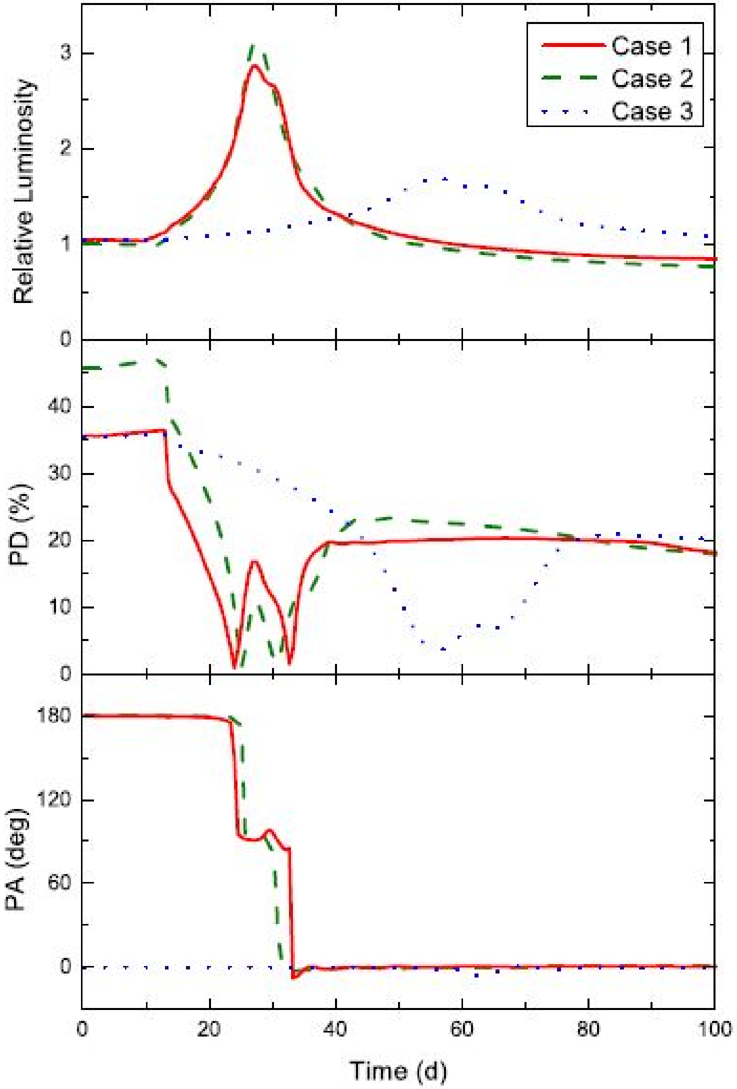

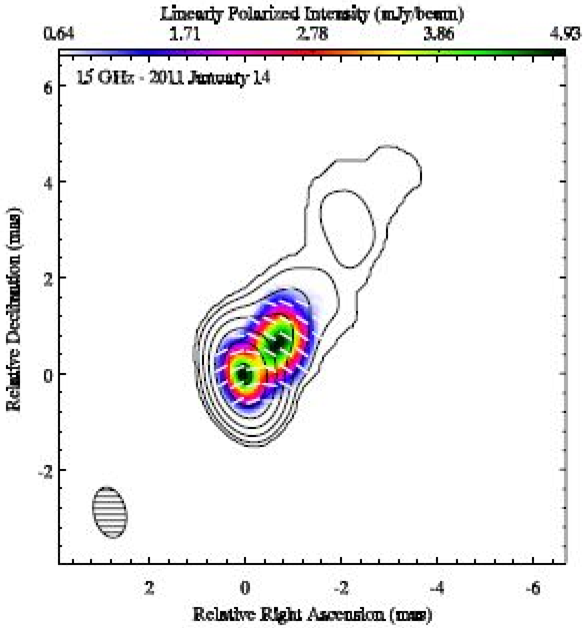

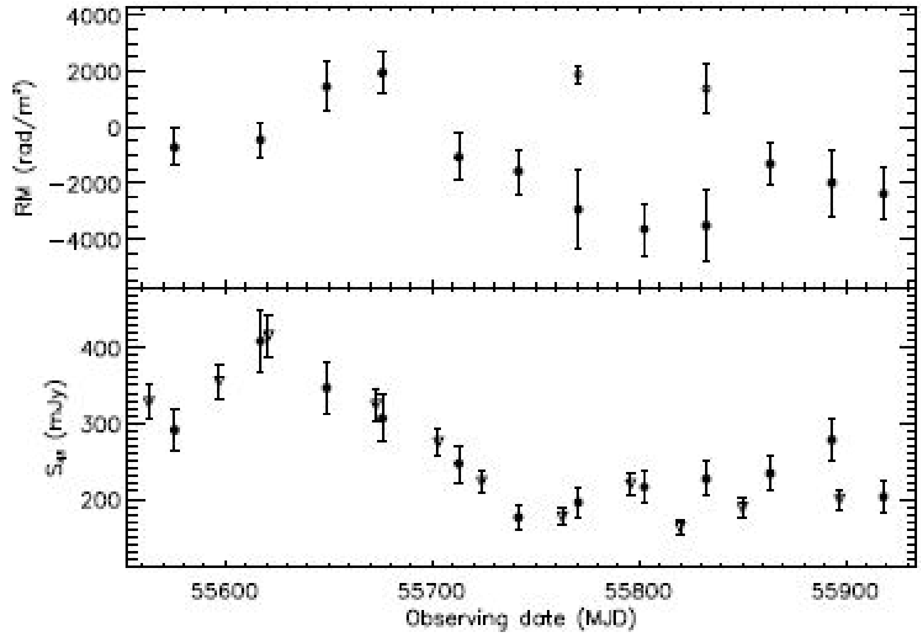

Lico, Gómez, Asada and Fuentes

“Interpreting the time variable RM observed in the core region of the TeV blazar Mrk 421”

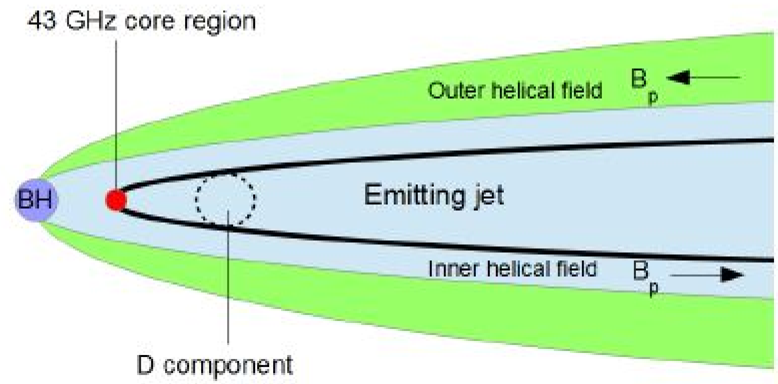

Figure 2. Schematic representation of the proposed magnetic tower model. The inner helical field (blue color) extends over the emitting jet region (solid black line), up to the jet sheath region, with $B_{\rm p}$ oriented in the observer's direction and producing a positive RM. The outer helical field (green color) has $B_{\rm p}$ pointing in the opposite observer's direction and produces a negative RM.

(3) New images and more on 3C 273

Tingdong Chen, Brandeis PhD thesis, 2005

Four epochs over nine months, 1999.26 – 2000.04,

observing at 8, 15, 22 and 43 GHz

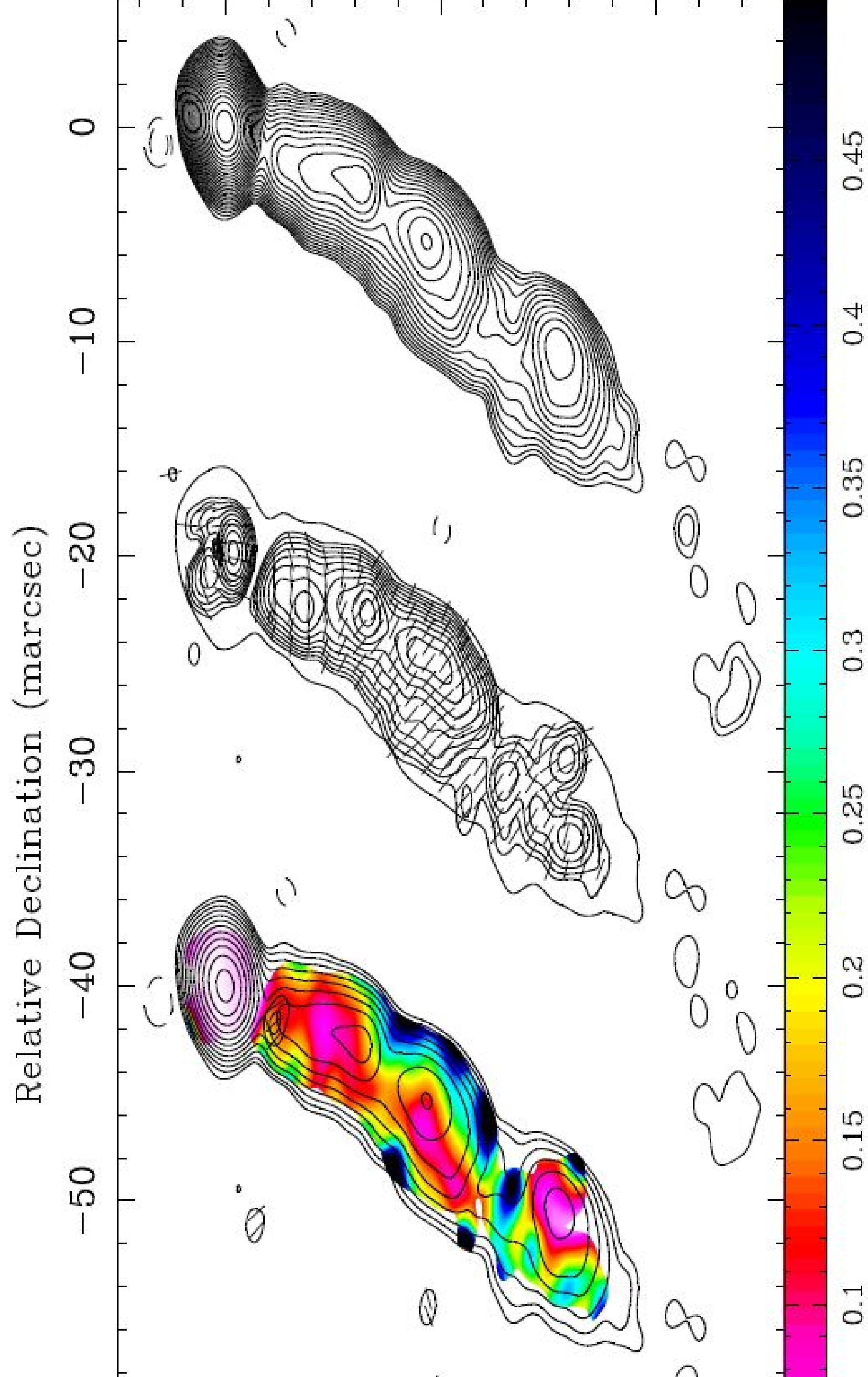

8 GHz images from 1999.37
top – I image
middle – P image with EVPA tick marks
bottom – fractional polarization (color) superposed on I contours

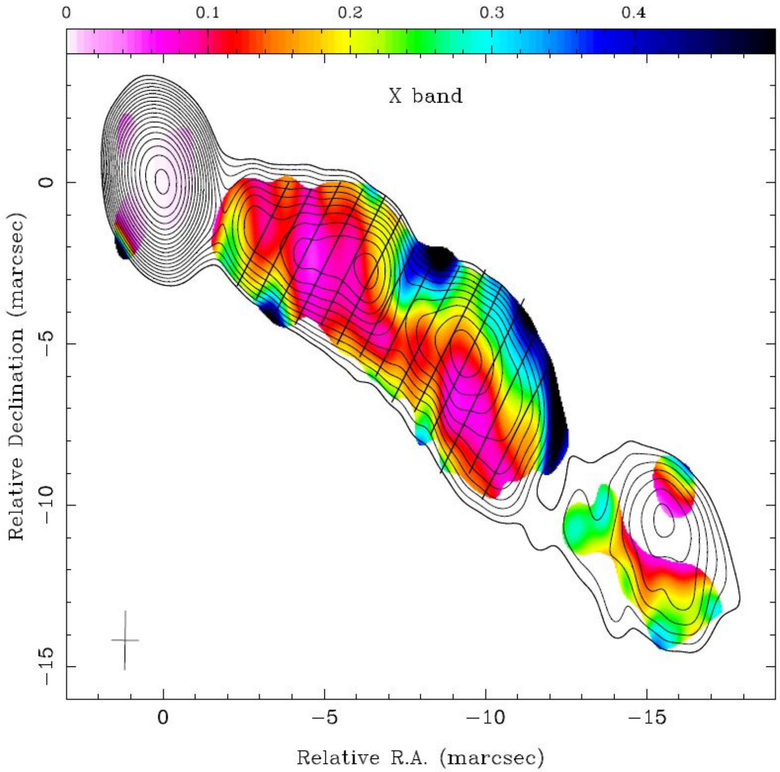

0
0.1
0.2
0.3
0.4
X band
Relative Declination (marcsec)
Relative R.A. (marcsec)
0
−5
−10
−15

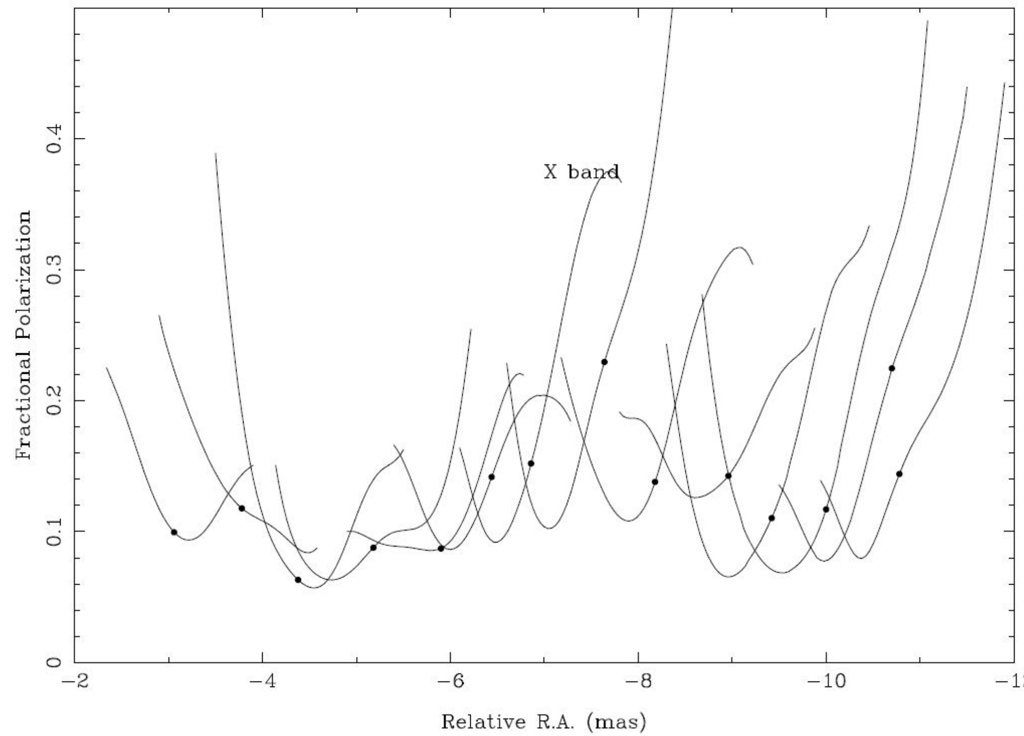

X band
Fractional Polarization
Relative R.A. (mas)
0
0.1
0.2
0.3
0.4
−2
−4
−6
−8
−10
−12

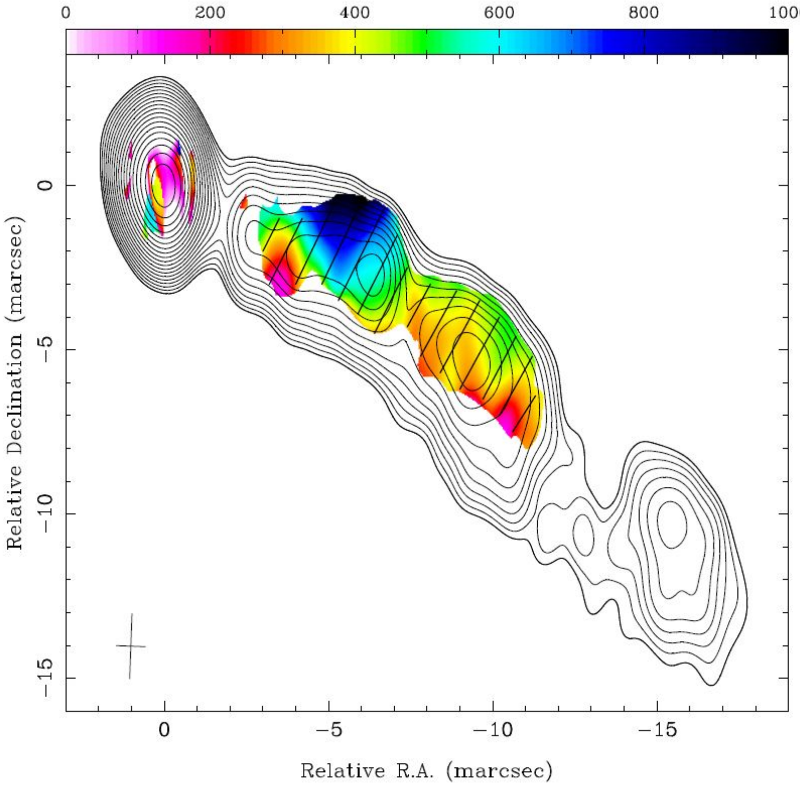

0
200
400
600
800
100
Relative Declination (marcsec)
0
−5
−10
−15
Relative R.A. (marcsec)
0
−5
−10
−15

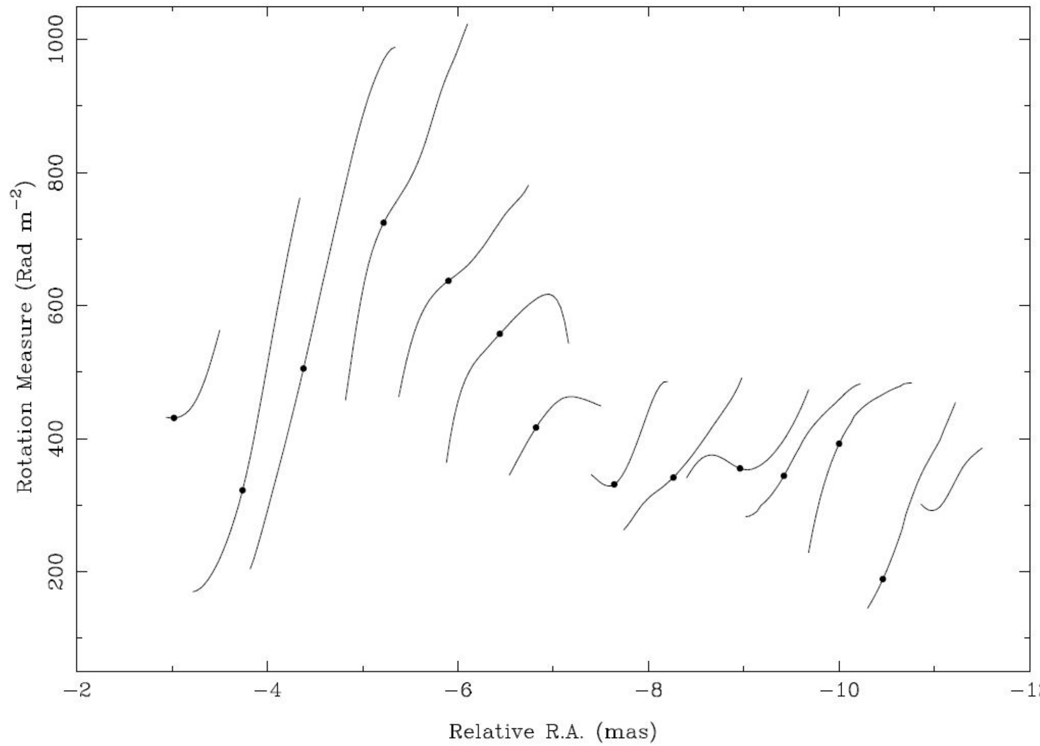

Rotation Measure (Rad m^{-2})
200
400
600
800
1000
Relative R.A. (mas)
−2
−4
−6
−8
−10
−12

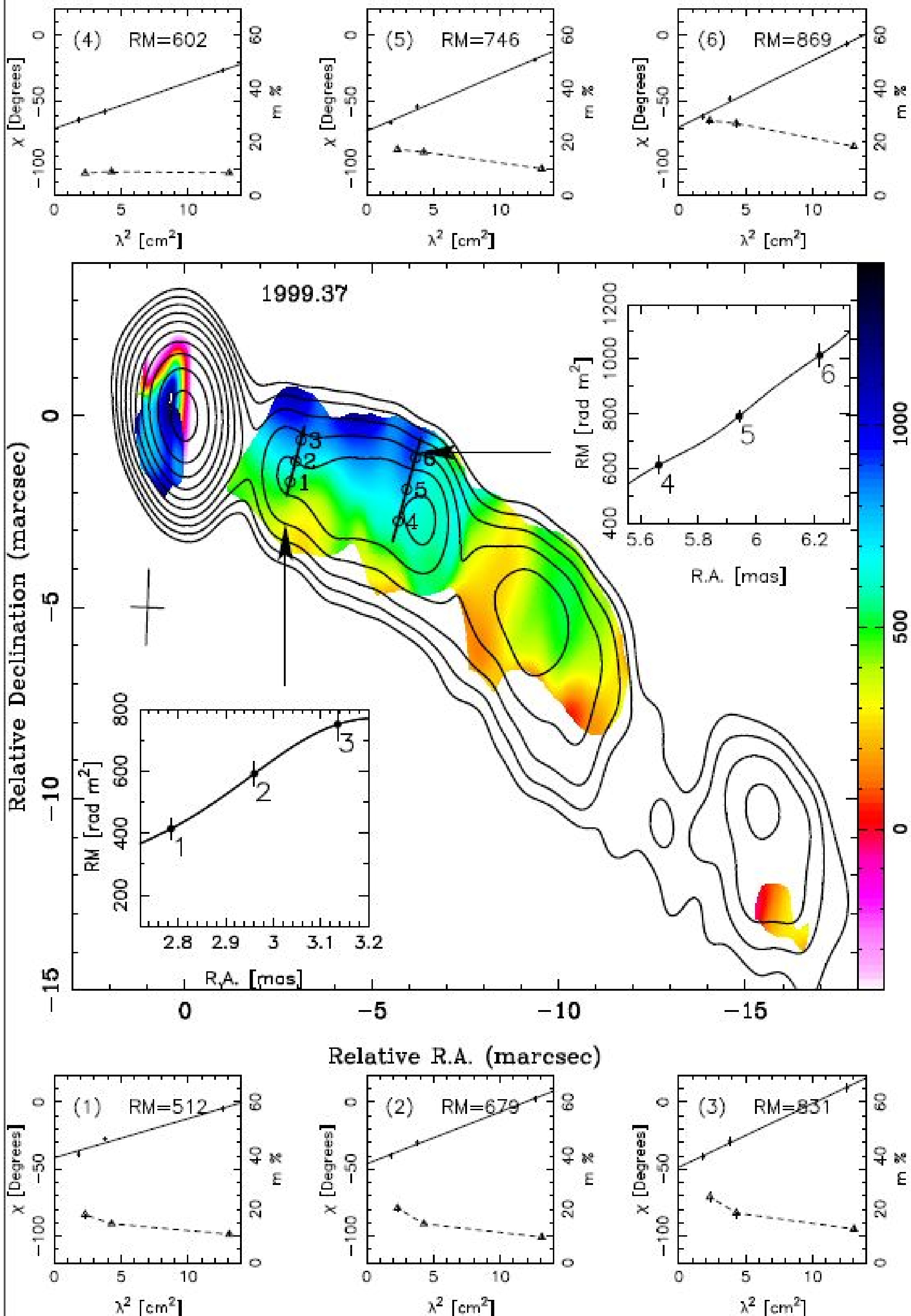
(4) RM=602
(5) RM=746
(6) RM=869
(1) RM=512
(2) RM=679
(3) RM=831
χ [Degrees]
m %
λ² [cm²]
1999.37
Relative Declination (marcsec)
Relative R.A. (marcsec)
RM [rad m⁻²]
R.A. [mas]

MID-POINT RM VARIABILITY:

Much larger amplitude,

Timescale = years

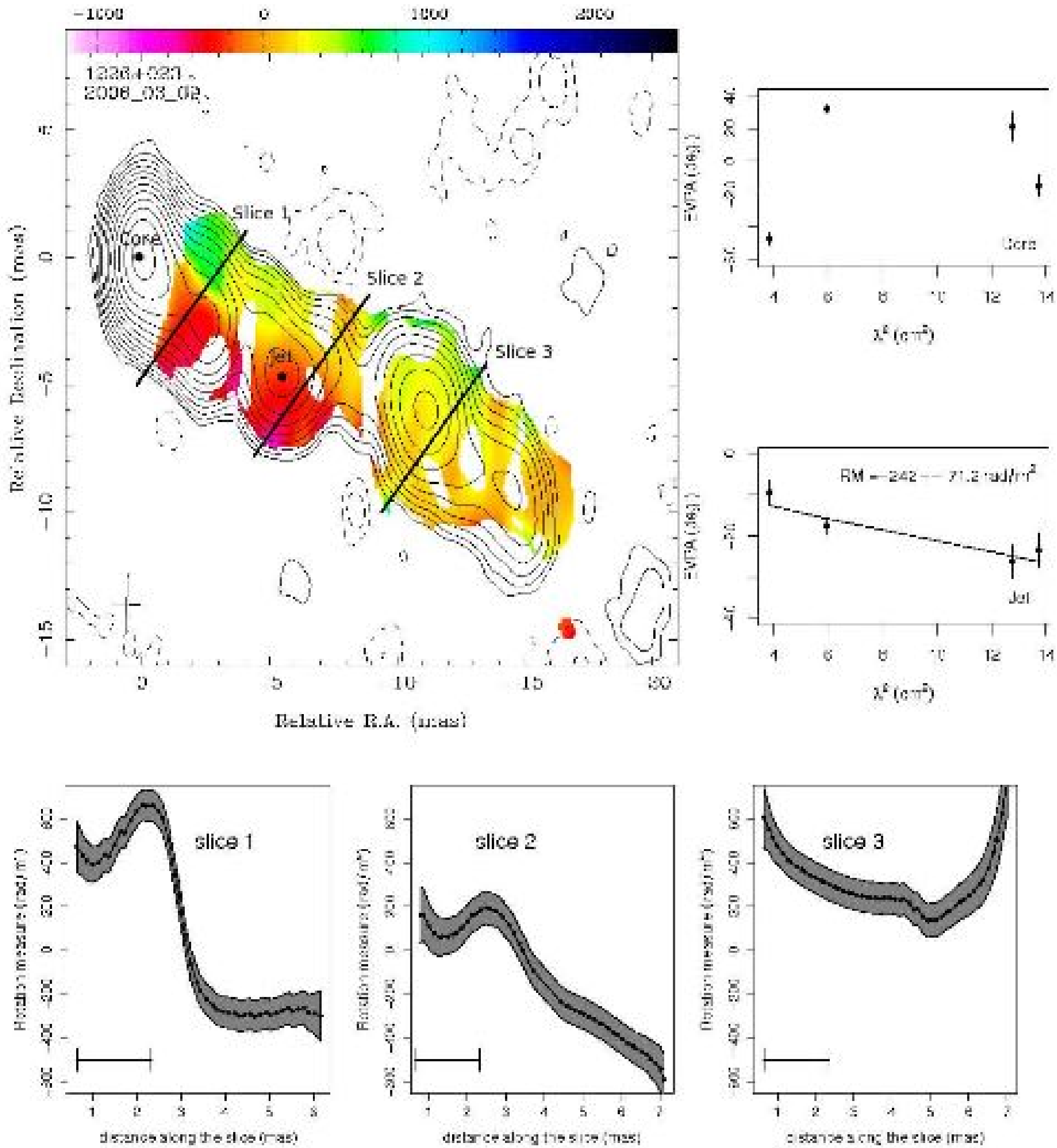

3C 273 pc-scale rotation measure observations

DATE	FREQ	Core-dist	**RM ridge**	RM gradient	REFERENCE
	GHz	mas	**rad/m^2**	rad/m^2/mas	
1995.92	4.7 - 8.6	6	**340**	60	Asada++2002
1997.07	8.1 - 43.2	5	**500**		Zavala & Taylor 2001
1999.26	8.1 - 22.2	3	**489**	185	Chen 2005
1999.26	8.1 - 22.2	6.5	**619**	61	Chen 2005
1999.37	8.1 - 22.2	3	**679**	207	Chen 2005
1999.37	8.1 - 22.2	6.5	**746**	160	Chen 2005
1999.74	8.1 - 22.2	3	**497**	170	Chen 2005
1999.74	8.1 - 22.2	6.5	**695**	211	Chen 2005
2000.04	8.1 - 22.2	3	**358**	137	Chen 2005
2000.04	8.1 - 22.2	6.5	**693**	213	Chen 2005
2000.07	8.1 - 43.2	5	**500**		Zavala & Taylor 2001
2000.07	12.1 - 22.2	5	**750**	600	Zavala & Taylor 2005
2000.61	12.1 - 22.2	5	**750**	600	Zavala & Taylor 2005
2002.35	43 - 86	0.8	**16000**	110000	Attridge++ 2005
2002.96	4.6 - 8.6	10	**400**	50	Asada & Inoue 2004
2002.96	4.6 - 8.6	14	**325**	35	Asada & Inoue 2004
2002.96	4.6 - 8.6	22	**200**	11	Asada & Inoue 2004
2006.19	8.1 - 15.3	3	**0**	450	Hovatta++ 2011
2006.19	8.1 - 15.3	8	**-100**	1600	Hovatta++ 2011
2006.19	8.1 - 15.3	13.5	**200**	125	Hovatta++ 2011

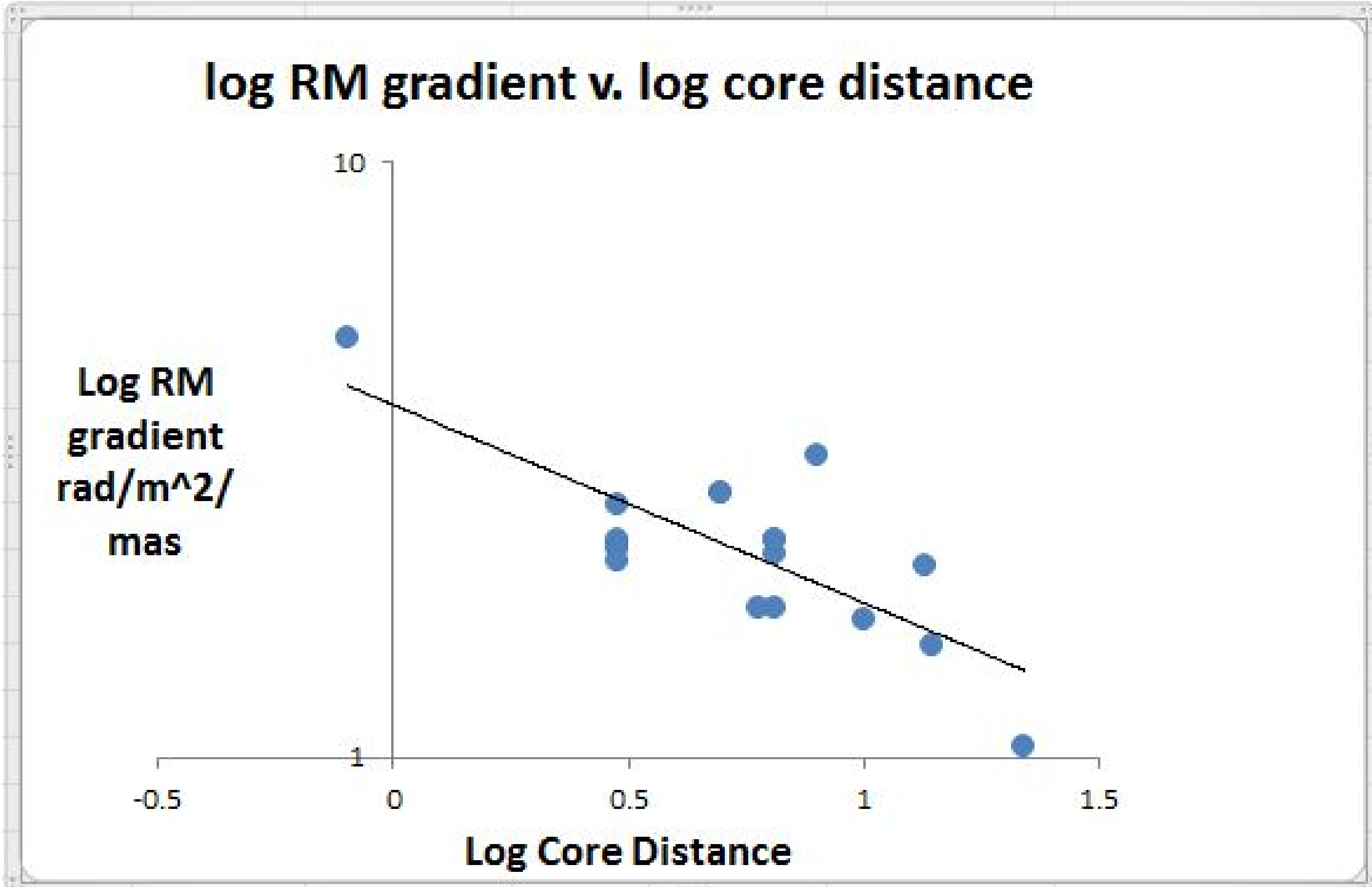

The gradient is variable and scales roughly as (core distance)^-2

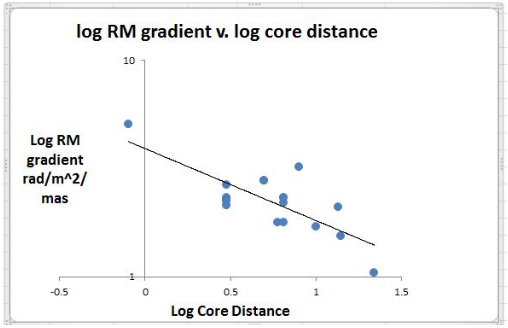

The ridge line RM is also variable on time scales of months to years. This may be due to moving jet components sampling different parts of the (very nearby) Faraday screen.

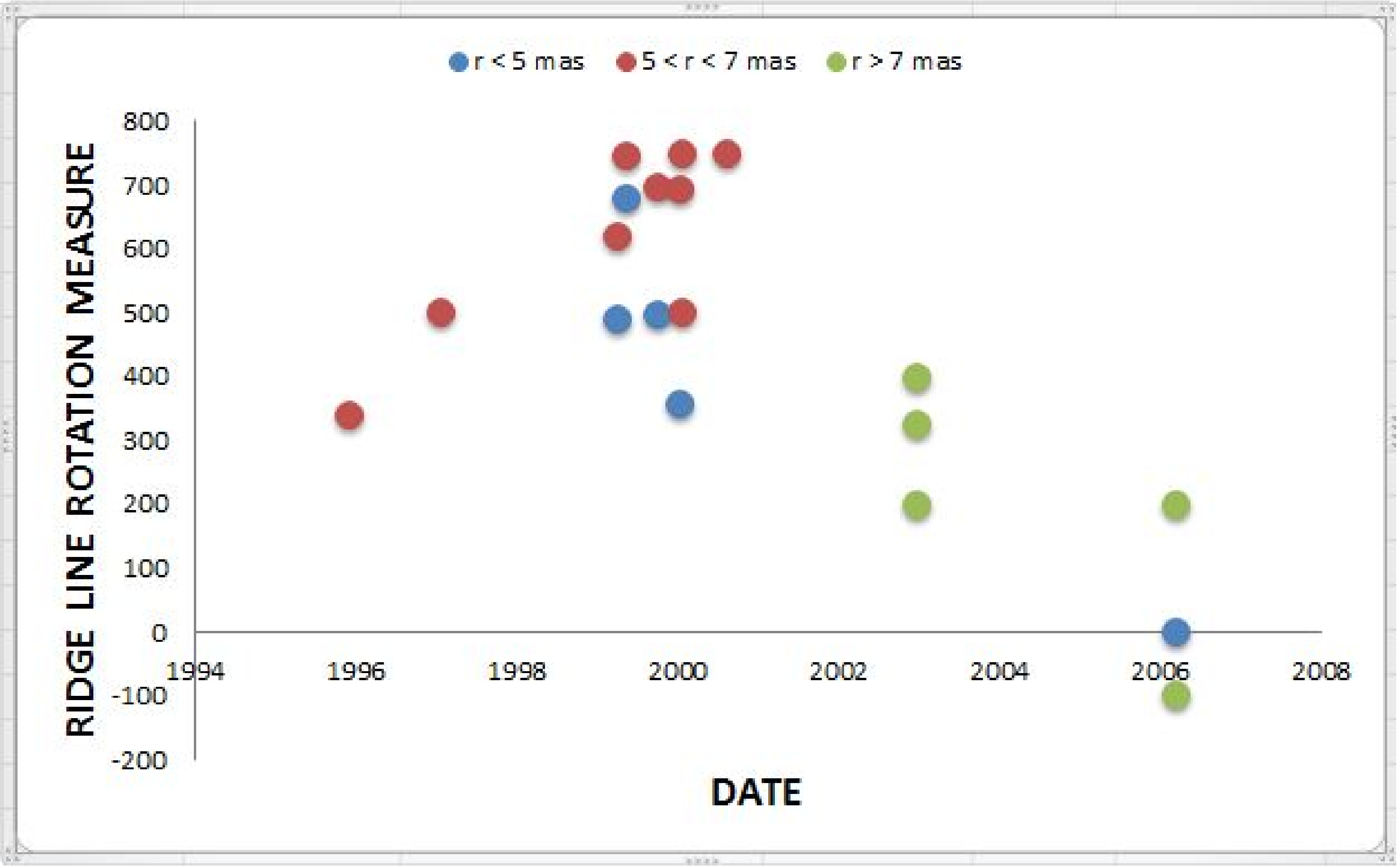

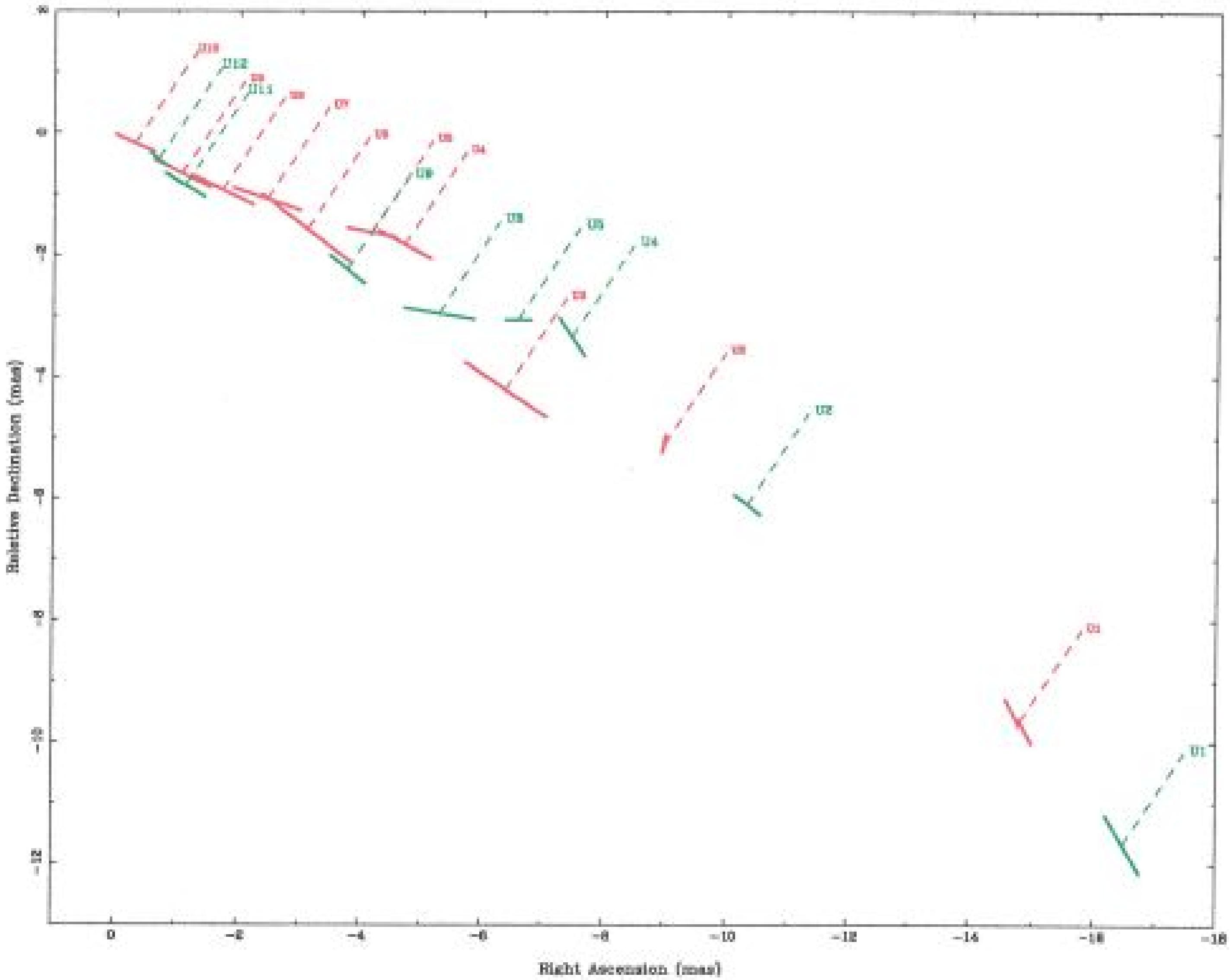

Figure 3.13: Plot components (U band) and proper motions together. Same symbols and colors for components as in Figure 3.12. The velocity vectors are plotted in different colors, red for 1996 epochs, and green for 1999 epochs.

MAGNETIC FIELD MODEL

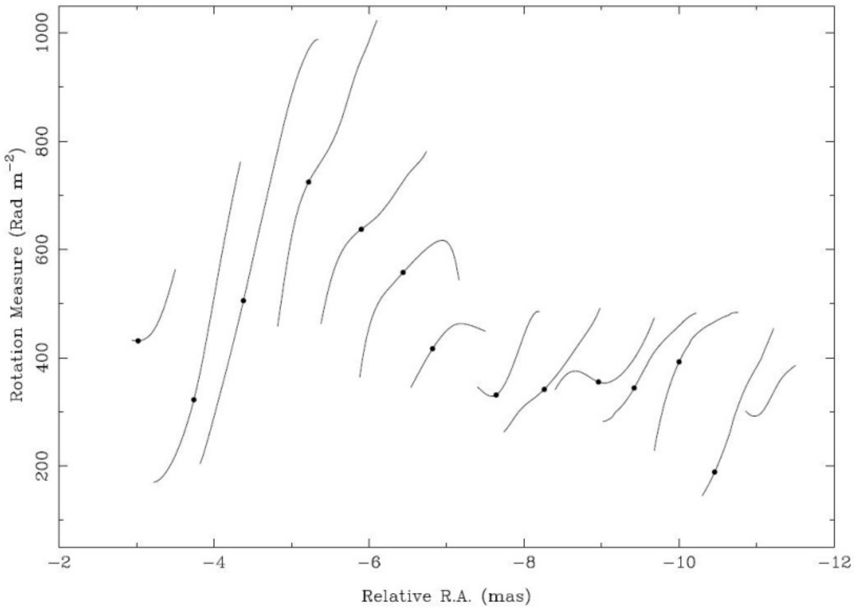

Here is a simple model for the magnetic field that may explain three persistent features:

(1) Transverse RM gradients
(2) Fractional polarization minimum in the center of the jet
(3) Net B field is longitudinal

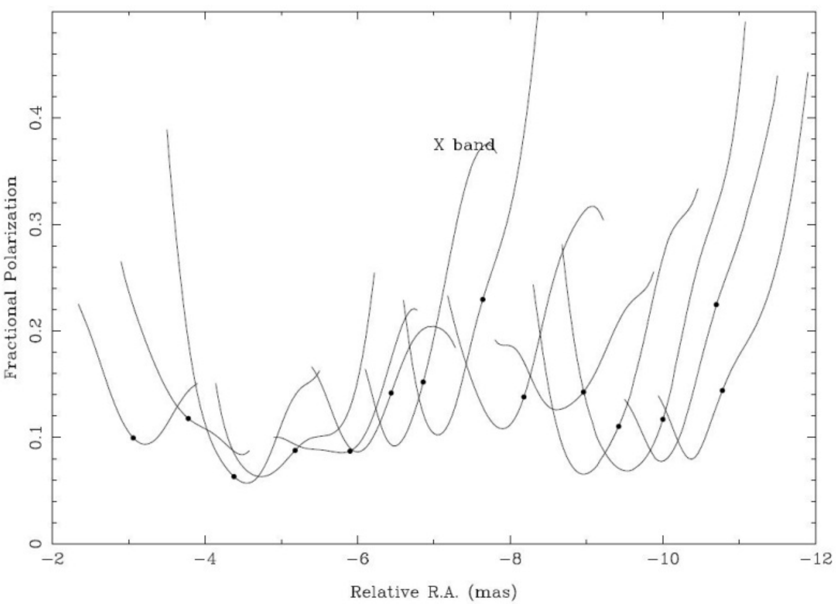

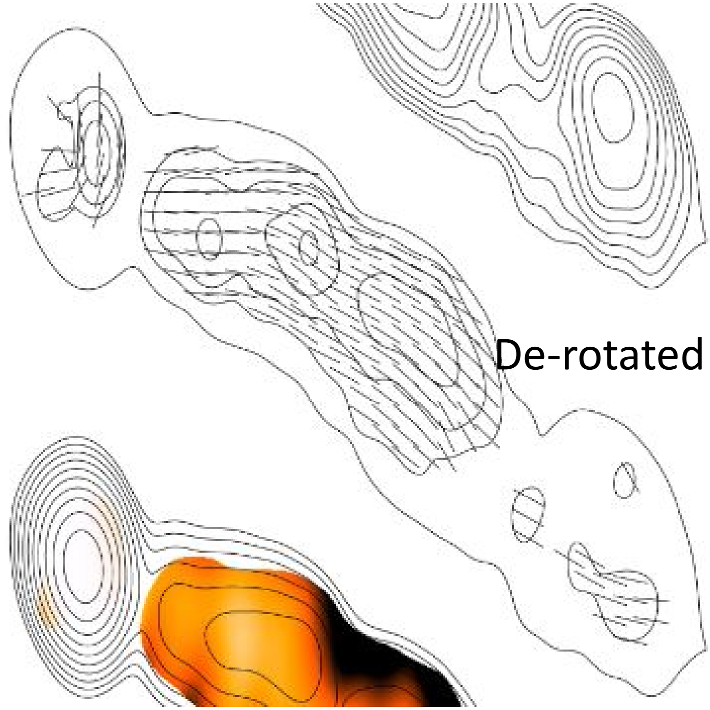

De-rotated “B vectors”

Jonathan Mizrahi, senior honors thesis, 2007

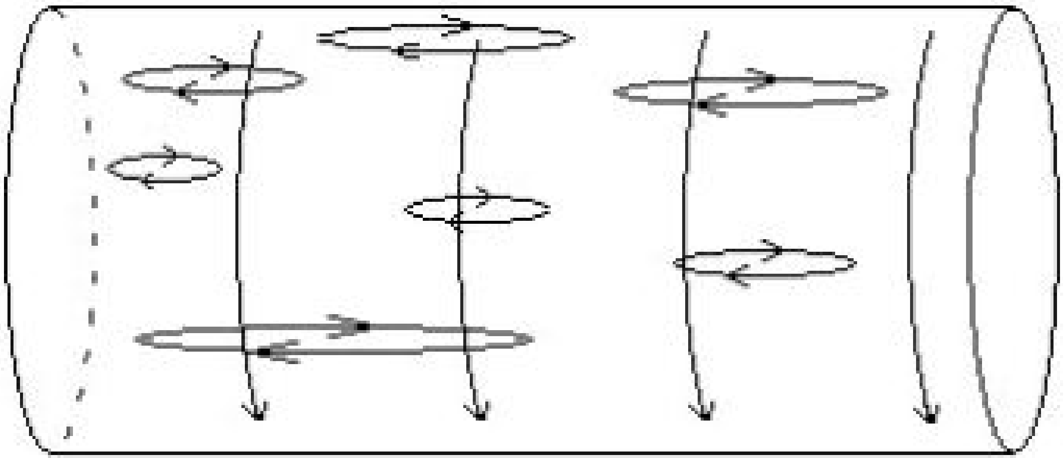

Figure 4: Model of magnetic fields

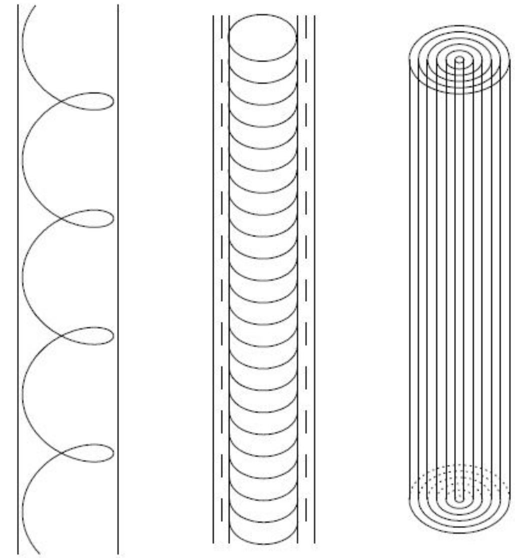

Fig. 2 Sketches of the three field configurations discussed in the text. Left: vector-ordered helix. *Middle*: perpendicular-field spine and longitudinal-field shear layer. *Right*: two-dimensional field sheets wrapped around the jet axis.

Laing, Canvin & Bridle 2006 and Laing 1980

The longitudinal field is not vector ordered. It therefore does not cause the transverse asymmetry intrinsic to a helical field (except at nd may avoid the conservation of flux problem. The loops may be continuously generated by boundary layer interactions plus a modest amount of shear.

Theta=9
00

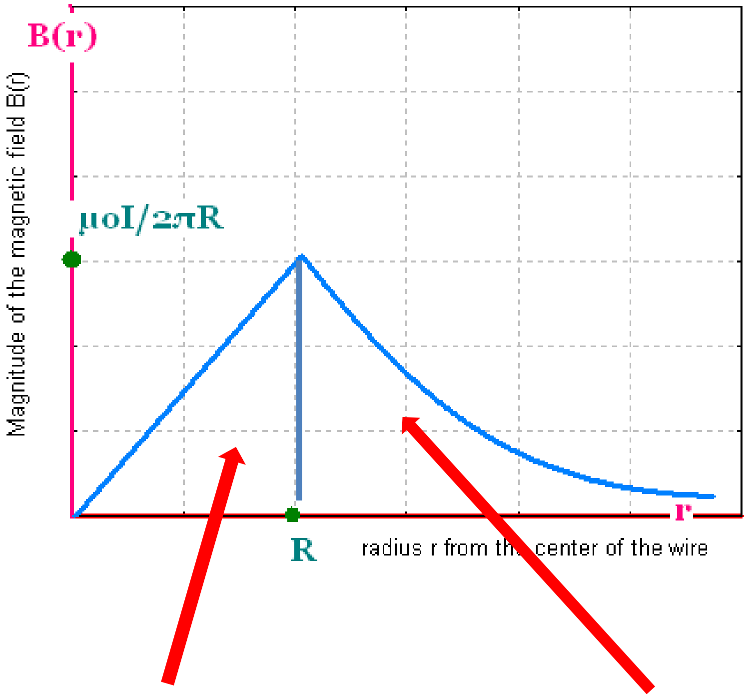

A toroidal component of the magnetic field requires that a current, I, flows down the jet (by Ampere's law) .

The graph on the left is for a uniform current density in a jet of radius R, carrying a total current I.

The field inside the jet gives rise to the observed synchrotron radiation, and probably to modest internal depolarization of the radiation.

The field outside of the jet is where nearly all the observed Faraday rotation occurs, including the RM gradient, in a sheath of plasma surrounding the jet. Moving VLBI components can map out the properties of the plasma.

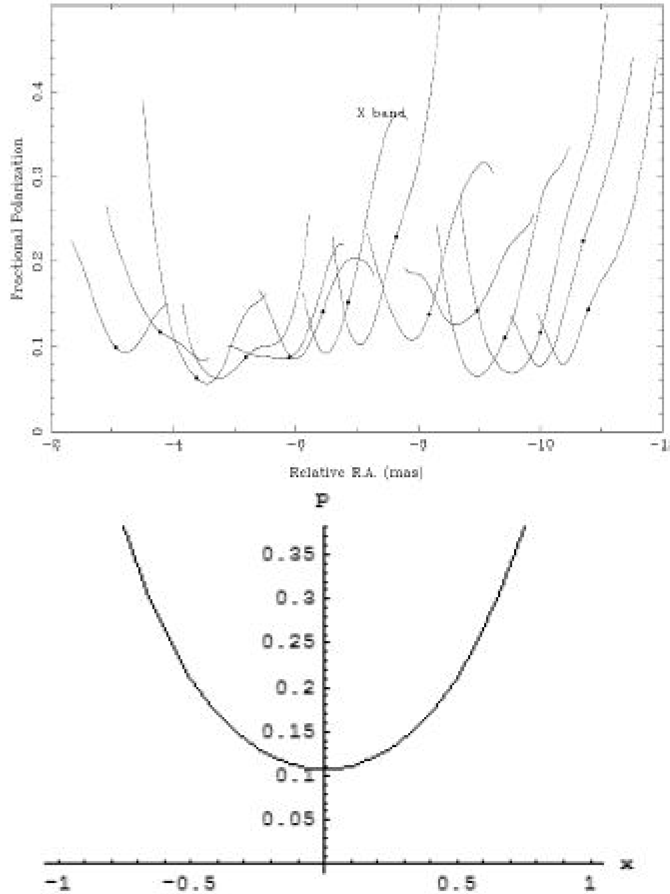

Figure 11: *Top*: Observed fractional polarization for different slices of 3C273. *Bottom*: Theoretical fractional polarization, with $b = 2/3$, $\theta = \pi/2$.

Here, b is the ratio of longitudinal field to toroidal field at the jet surface.

CURRENTS IN JETS

The current is given by $I = \dfrac{2\pi R_{jet}\, B_{tor}}{\mu_0}$

The median value of the magnetic field from core-shift measurements is 1 G at 1 pc. (e.g. Pushkarev ++ 2012)

The median intrinsic jet opening angle is 1.3^{o} (e.g. Pushkarev ++ 2017)

These then give a typical jet current $I \sim 2 \text{ x } 10^{17}$A

Kronberg ++ 2011 have measured the current in a *Kpc –scale jet*, in the radio galaxy 3C 303, also using an observed RM gradient. Jet knot C/E3 is about 20 kpc from the nucleus, and they determine a value for the current of $I \sim 4 \text{ x } 10^{17}$A.

Here, as in 3C273, the conventional current is away from the nucleus, so if the charge carriers are electrons, they flow down the jet *towards* the nucleus.

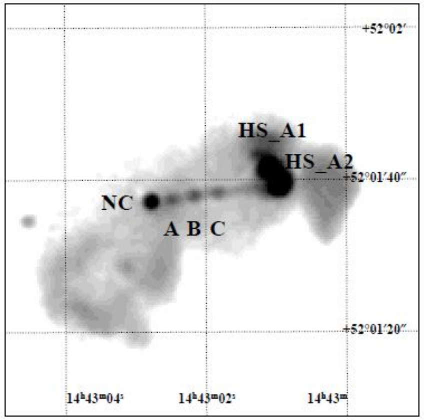

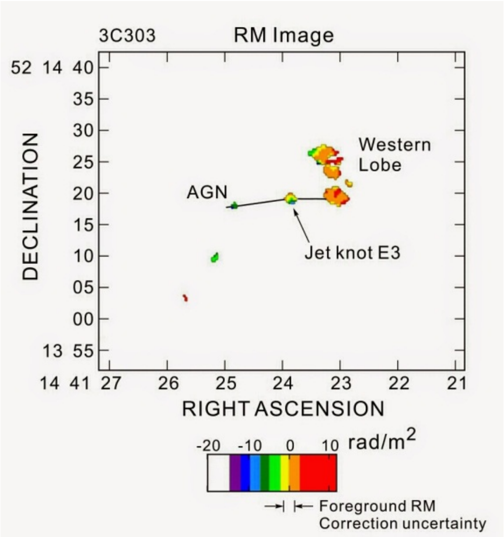

Fig. 3.— Faraday rotation image of the 3C303 radio source at a resolution of 1.5″. The RM zero level has been corrected by 18 ±4 rad m^{-2} (see text).


Thank you for your attention,
Ευχαριστώ
And thanks to the organizers for this very excellent meeting